

# Supramolecular Chiral 2D Materials and Emerging Functions

Bowen Shen, Yongju Kim,\* and Myongsoo Lee\*

Chiral materials are widely applied in various fields such as enantiomeric separation, asymmetric catalysis, and chiroptical effects, providing stereospecific conditions and environments. Supramolecular concepts to create the chiral materials can provide an insight for emerging chiro-optical properties due to their well-defined scaffolds and the precise functionalization of the surfaces or skeletons. Among the various supramolecular chiral structures, 2D chiral sheet structures are particularly interesting materials because of their extremely high surface area coupled with many unique chemical and physical properties, thereby offering potential for the next generation of functional materials for optically active systems and optoelectronic devices. Nevertheless, relatively limited examples for 2D chiral materials exhibiting specific functionality have been reported because incorporation of molecular chirality into 2D architectures is difficult at the present stage. Here, a brief overview of the recent advances is provided on the construction of chiral supramolecular 2D materials and their functions. The design principles toward 2D chirality and their potential applications are also discussed.

readily recovered with higher recyclability and hence attract broader research interests.<sup>[6,7]</sup> Thus far, through building blocks and linkages in a proper design, a series of chiral supramolecular architectures have been developed for the use as chiral catalysts or enantiomeric separations.<sup>[8,9]</sup>

To this end, much research efforts have been devoted to produce the supramolecular chiral materials with superior properties; however, the efficiency in applications is relatively limited, suffering from the low conversion yield or low enantioselectivity in most cases.<sup>[10,11]</sup> Among these, two typical supramolecular chiral structures with different dimensions are widely investigated, i.e., 1D and 3D structures. In the case of 1D structures such as helical fibers and chiral tubules, a lack of internal cavities or easy deformation of the elongated internal cavities hinder their precise applications.<sup>[12,13]</sup>

## 1. Introduction

Chiral materials have attracted tremendous attention from the research communities across chemistry, material science, biology, and physics in recent decades and have shown significant development for diverse potential applications including signal amplifications, asymmetric synthesis, and optical devices.<sup>[1–5]</sup> A typical example is the acquisition of chiral organic compounds, in particular the chiral drugs, by direct synthesis via chiral catalysts or resolution of racemic mixtures. Unlike the homogeneous catalyst at molecular level, the supramolecular chiral architecture-based heterogeneous catalysts can be

While the 3D structures (bulk materials), such as chiral zeolites and chiral organic frameworks, have been utilized in many fields, most of them are subjected to precipitation and are rarely organized in unidirection (homochirality) due to the high-temperature calcination or multidomain organizations.<sup>[14]</sup> In this respect, the 2D structures having an intrinsic platform to endow chiral properties are considered as a promising candidate to overcome the limitations of 1D and 3D materials. It is noteworthy that one of the unique structural features of 2D materials enables the chiral materials to exhibit an extremely large surface-to-volume ratio and good dispersibility in solution. Recently, numerous studies have shown that 2D materials have distinctive properties compared with 3D bulk materials. As a well-known example, graphene, has motivated widespread research efforts on 2D materials and thus witnessed the “2D material gold rush”. The 2D graphene, compared with its 3D form of graphite, shows a much higher carrier mobility and mechanical flexibility.<sup>[15,16]</sup> Nevertheless, despite the success in the construction of chiral materials, it still remains a critical challenge to synthesize the 2D materials with permanent or switchable chirality which simultaneously exhibit good solubility and stability. Two emerging 2D materials such as 2D metal organic frameworks (MOFs) and 2D covalent organic frameworks (COFs) have been modified to induce chirality; however, some of the exfoliated sheets still spontaneously restack due to poor solubility and eventually form bulk 3D materials.<sup>[17]</sup> For this reason, several approaches are developed to avoid the aggregation of the sheets and maintain stable 2D layered materials. These include self-assembly of amphiphiles,<sup>[18,19]</sup> peptide assembly,<sup>[20,21]</sup> host–guest interactions,<sup>[22]</sup> and

Dr. B. Shen, Prof. M. Lee  
State Key Lab of Supramolecular Structure and Materials  
College of Chemistry  
Jilin University  
Changchun 130012, China  
E-mail: mslee@jlu.edu.cn

Prof. Y. Kim  
KU-KIST Graduate School of Converging Science and Technology  
Korea University  
Seoul 02841, Republic of Korea  
E-mail: yongjukim@korea.ac.kr

Prof. M. Lee  
Department of Chemistry  
Fudan University  
Shanghai 200438, China

 The ORCID identification number(s) for the author(s) of this article can be found under <https://doi.org/10.1002/adma.201905669>.

DOI: 10.1002/adma.201905669

postmodification.<sup>[23]</sup> Taking advantage of the reduction in thickness, the substrates can be efficiently and reversibly bound to and released from the 2D chiral materials. The properties of the material are highly depending on their structural topologies and chiral functional moieties, which therefore determine their suitability for different applications.<sup>[24,25]</sup>

Recent reviews have covered some synthetic methods and applications with COFs and MOFs materials based on covalent bonds and metal coordination bonds, respectively;<sup>[26–28]</sup> however, it is still lacking a comprehensive overview for the recent advances of 2D chiral sheet materials based on not only covalent bonds or coordination bonds but also noncovalent supramolecular interactions, especially for those studies that explore the optical activity of achiral building blocks in chiral nanostructures. Herein, the construction of supramolecular 2D architectures will be first introduced, followed by discussing the latest advances of the pure or porous chiral 2D materials, and finally providing further directions for designing the supramolecular chiral 2D materials will be suggested.

## 2. 2D Supramolecular Materials

The first obstacle to construct 2D chiral sheet materials is how to prevent 3D stacks of the individual layers. Regardless of surface area, the huge surface energy has high potential to drive sheet architectures to stack and, consequently, to form irregular precipitates. In most cases, two distinct strategies have been introduced to construct 2D architectures: “bottom-up” strategy in which sheet architectures are synthesized directly from small building blocks via different interactions and “top-down” strategy in which sheet architectures are stripped from bulk layered materials.<sup>[29]</sup>

### 2.1. 2D Materials from Top-Down Strategy

2D graphene derivatives have been developed by postmodifications to exhibit extraordinary electronic, optical, magnetic, thermal, and mechanical properties.<sup>[30]</sup> Due to the property of the starting materials “graphite”, top-down strategy such as mechanical cleaving<sup>[31]</sup> and chemical exfoliation is compatible to ultrathin graphene preparation.<sup>[32]</sup> Among the many exfoliation techniques, dissolution of graphite into solvents such as dimethylformamide is one of the most commonly used methods today. In addition, aromatic surfactant molecules in aqueous solution provide an alternative strategy for exfoliation graphite powder into single- and double-layer graphenes. Lee et al. synthesized an oligoether dendron grafted to a conformationally flexible aromatic segment including four pyrene moieties. The hydrophilic functionalization of graphene surfaces through combination of amphiphilicity and  $\pi$ - $\pi$  stacking interactions between the graphene surfaces and the aromatic amphiphiles induces ultrathin graphene dispersions (Figure 1a). When the graphene surfaces are covered by hydrophilic chains, the graphene sheets show to be very stable in aqueous solution without precipitation or aggregation even after centrifugation or standing over 2 months.<sup>[33]</sup>

### 2.2. 2D Materials from Bottom-Up Strategy

Inspired by above results, hydrophilic moieties with bulky steric effect provide an opportunity to stabilize high surface energy of 2D architectures. The self-assembly process of amphiphiles in aqueous solution is the “bottom-up” strategy in which amphiphilic building blocks can form 2D architectures spontaneously via defined design of the hydrophilic oligoether chains and hydrophobic aromatic segments. A series of 2D flatten architectures have been constructed by cisoid stacking patterns of bent-shape aromatic amphiphiles and lateral association of the nanofibers from macrocyclic amphiphiles.<sup>[19,34]</sup> In addition to the building blocks that spontaneously form free-standing 2D-self-assemblies in solutions, a fixed planar surfaces can be used as a substrate to guide the 2D self-assembly of building blocks on the 2D substrate through various interactions. According to this strategy, electrostatic interactions provide an opportunity to construct sheet nanostructures on a pre-existed substrate surface. Recently, Lee group constructed supramolecular sheets via self-assembly of aromatic rods with carboxylate group. The atomic force microscopy (AFM) experiments showed that the sheets are stable with homogeneous thickness of 2.8 nm, indicating that the aromatic segments pack in a monolayer arrangement with carboxylate-coated surfaces. The carboxylate-coated surfaces can be used as a template to guide spreading of positively charged macrocycle objects on the 2D surfaces via electrostatic interactions. Indeed, in acidic condition (pH = 5.5), the negative-charged planar sheets can guide electrostatic spreading of the partially positive-charged macrocycles on the surface to generate dynamic 2D honeycomb heterostructures (Figure 1b)<sup>[35,36]</sup> Upon manipulating the lateral associations through the strength of aromatic interactions will lead the resulting planar sheet to form porous sheets.<sup>[37]</sup> To further control the dynamic response characteristics of the pore, a flat aromatic bicycle segment was synthesized with an oligoether dendron grafted at the center of the basal plane to frustrate layer-to-layer stacking.<sup>[38]</sup> Porous sheets protected by the hydrophilic chains are formed through lateral association of amphiphile dimers with an average pore size of 3.5 nm and shown to be highly stable in solution (Figure 1c). Notably, the pores are able to undergo open-closed switching driven by guest intercalation. When the dimers adopt fully overlapped packing driven by flat aromatic intercalation, the porous sheets transform into closed sheets reversibly due to enhancement of lateral aromatic interactions.

Rigid molecules with macrocyclic topology can provide appropriate building blocks for construction of 2D sheet structures through noncovalent interactions. For example, the development of the pillar[*n*]arenes with a permanent pore provides a platform to construct 2D architectures with various functions via tuning interaction between pillar[*n*]arenes and guest molecules.<sup>[39]</sup> In the case of pillar[6]arene P[6]1, when some hydroquinone units of P[6]1 were oxidized to benzoquinones, the formation of charge-transfer complexes would induce a side-by-side arrangement and form hexagonal dense packing of p[6]1.<sup>[40]</sup> In the presence of polyoxometalate (POM), the porous sheets were observed from the self-assembly of imidazolium-functionalized pillar[6]arene P[6]2. Under the premise of sacrificing hexagonal order, sheets can be stabilized, which shows

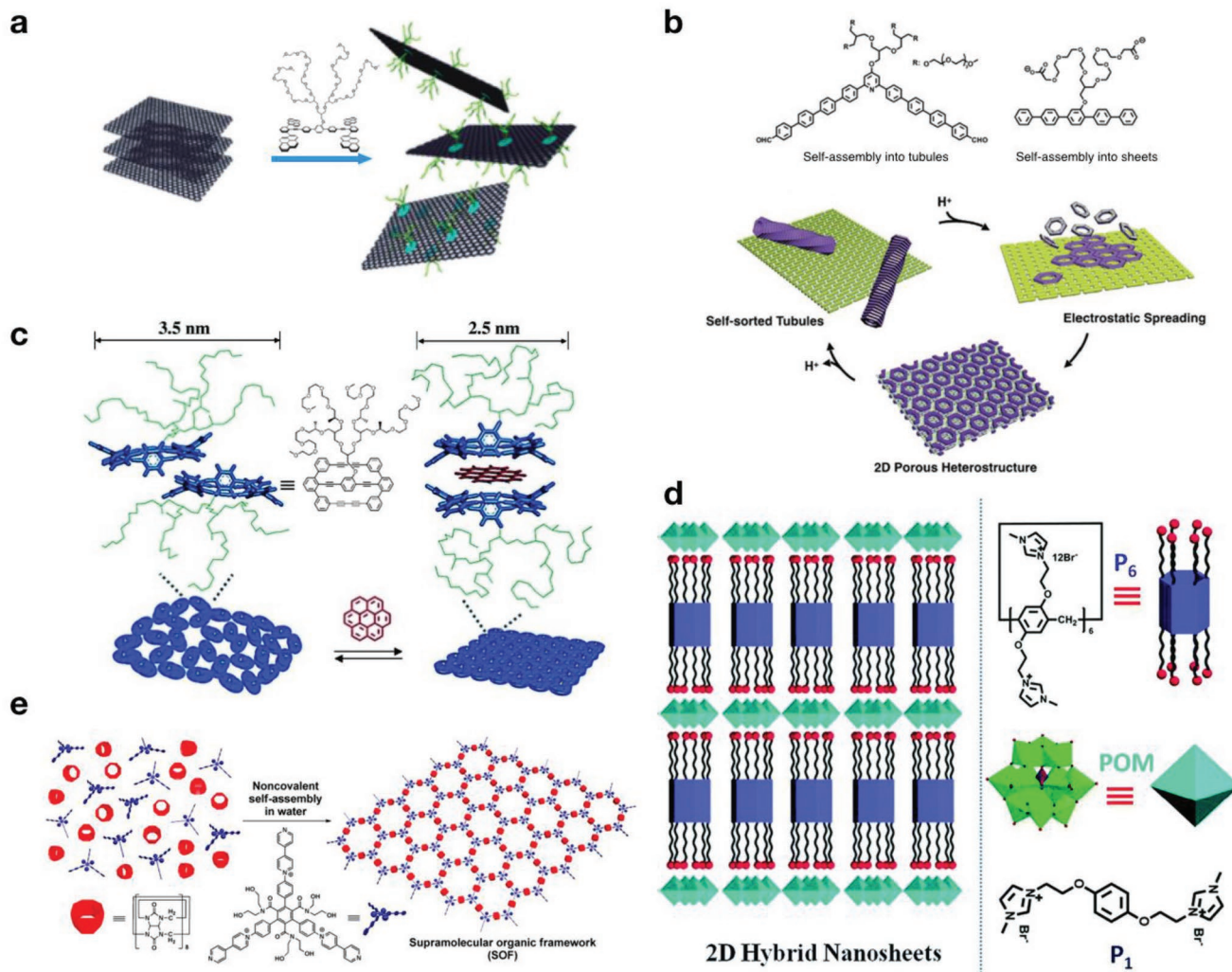


**Figure 1.** Schematic representation of construction of supramolecular 2D architectures. a) Selectively exfoliation of graphite powder into single- and double-layer graphene sheets in aqueous solution through hydrophilic functionalization of graphene surfaces. Reproduced with permission.<sup>[33]</sup> Copyright 2011, Royal Society of Chemistry. b) A hierarchical spreading of the stacked macrocycles of nanotubes on the surfaces of a self-sorted sheet materials. Reproduced with permission.<sup>[35]</sup> Copyright 2018, Royal Society of Chemistry. c) Lateral association of amphiphile dimers into a 2D structure with nanosized lateral pores and open-closed switching of pores. Reproduced with permission.<sup>[38]</sup> Copyright 2013, Wiley-VCH. d) 2D hybrid nanosheets from self-assembly of P[6]2 and POM via the electrostatic interaction and lateral association. Reproduced with permission.<sup>[41]</sup> Copyright 2018, Royal Society of Chemistry. e) A single-layer 2D supramolecular organic framework (SOF) by the tunable complexation between CB[8]- and BP-containing aromatic guests. Reproduced with permission.<sup>[43]</sup> Copyright 2013, American Chemical Society.

property of speeding up the degradation of dye molecules (Figure 1d).<sup>[41]</sup>

Despite of the successful instances of sheet architectures, construction of soluble single-layer sheets with ordered pore arrangement is rarely reported. Surface self-assembly and polymerization may provide the solutions to form single-layer sheets; however, the difficulty of exfoliation while maintaining the sheet structures limits the practical applications.<sup>[42]</sup> In 2013, Li and co-workers reported an excellent example of soluble, well-defined 2D supramolecular polymers via host-guest complexes between rigid 1,3,5-triphenylbenzene derivative and cucurbit[8]uril (CB[8]).<sup>[43]</sup> The strong complexation of CB[8] with two 4,4'-bipyridin-1-ium (BP) units of adjacent molecules stabilized this solution-phase single-layer 2D supramolecular organic frameworks (SOFs). The dynamic light scattering and

solution-phase small-angle X-ray scattering experiments demonstrated the hexagonal pores with uniform diameter of 3.7 nm (Figure 1e). This excellent strategy paves the way of construction 2D architectures with periodic porous organization that are finely dispersed in solution.<sup>[44,45]</sup>

### 3. Introducing Chirality into 2D Sheet Structures

Inspired by the development of 2D architectures, endowing chirality into 2D materials has attracted scientists' intense interests due to additional properties including chiroptical responses and enantiomer selective recognition. To give an overview of chiral 2D sheet materials, three most well-known strategies are introduced: direct synthesis, chiral induction synthesis, and postmodification.

### 3.1. Direct Synthesis

This strategy utilizes chiral building blocks to form 2D chiral supramolecular skeletons. The chirality of the building blocks will preserve in the next level architectures without racemization. A typical example is provided by peptide assembly in which the building blocks have the inherent chirality of their backbones.

In 2016, Lee and co-workers reported switchable chiral supramolecular objects formed through short  $\alpha$ -peptide assembly that undergo reversible switching via thermal treatment between assembly and disassembly states (Figure 2a). The peptide building block consists of a KKK(FAKA)<sub>3</sub>FKKK amino acid sequence and two oligoether dendrons as a side chain which are symmetrically grafted into the peptide backbone via click

reaction. Upon heating, the thermal dehydration of the oligoether chains induces the peptide with a random conformation to adopt an  $\alpha$ -helix conformation. The conformational switching into an ordered conformation gives rise to self-assembly of peptide building blocks into 2D disks architectures which were confirmed by cryogenic transmission electron microscopy and AFM experiments. Due to the helicity of the peptide units, the membrane structures have high potential to be utilized for chiral separation. Indeed, vesicular nanostructures formed from the same peptide backbones showed enantioselective separation of racemic 1-(4-bromophenyl)-ethanol.<sup>[46]</sup> In the same year, Rauschenbach group also reported 2D network with highly ordered hexagonal pores through self-assembly of oligopeptides.<sup>[47]</sup> Scanning tunneling microscopy reveals changes from compact or linear assemblies to long-range ordered, chiral

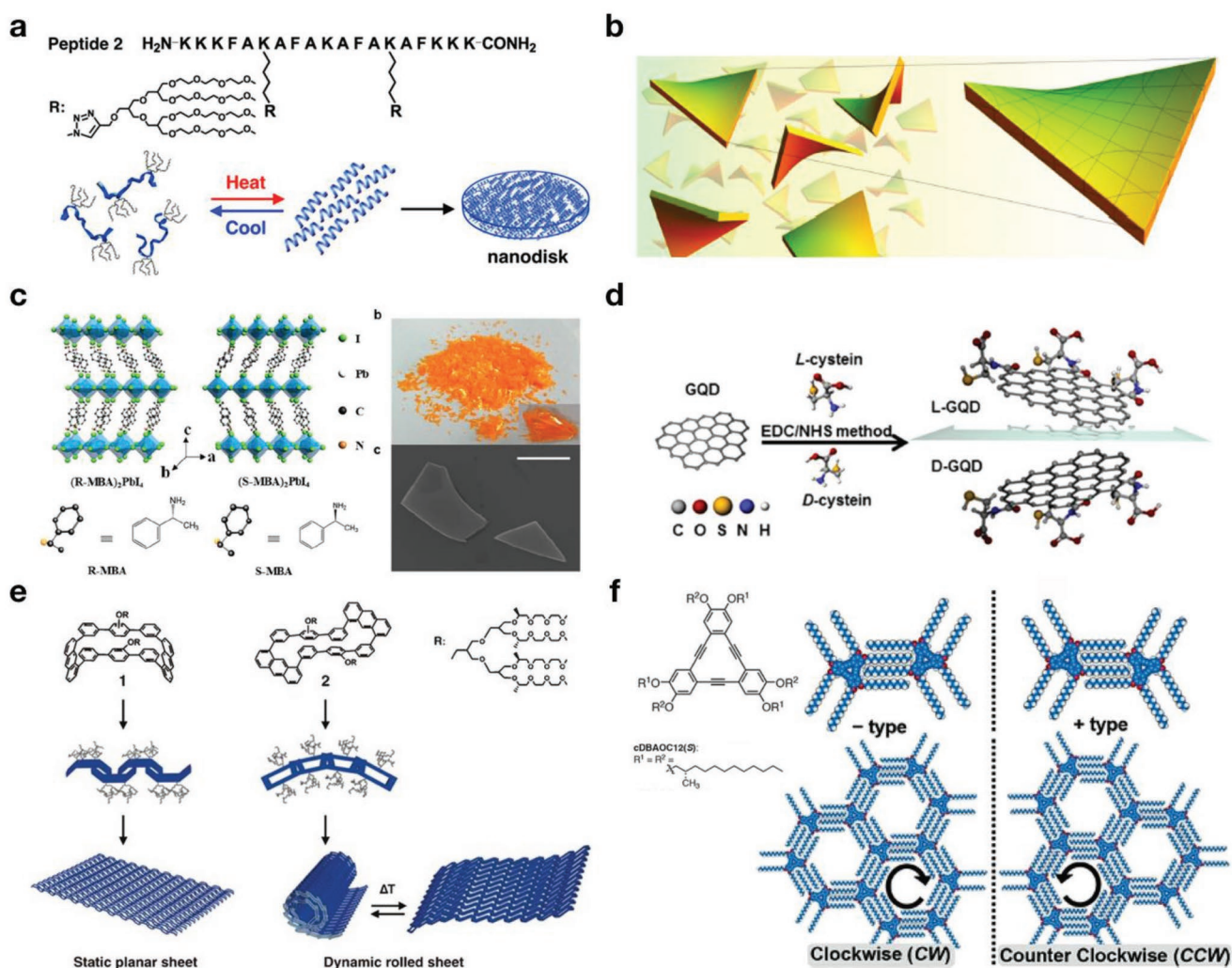


**Figure 2.** Schematic representation of chiral sheets. a) Switchable chiral membrane through  $\alpha$ -helical peptides between assembly and disassembly states by thermal trigger. Reproduced with permission.<sup>[46]</sup> Copyright 2016, American Chemical Society. b) Induced chiral sheets by liquid exfoliation of MoS<sub>2</sub> in the presence of chiral ligands (cysteine and penicillamine). Reproduced with permission.<sup>[51]</sup> Copyright 2018, American Chemical Society. c) 2D chiral perovskites with a high degree of the circularly PL by incorporating the chiral ligands. Reproduced with permission.<sup>[53]</sup> Copyright 2019, American Chemical Society. d) Chiral graphene through covalent attachment of L/D-cysteine to the edges of graphene quantum dots (GQDs). Reproduced with permission.<sup>[59]</sup> Copyright 2016, American Chemical Society. e) Static and dynamic chiral sheets from selective self-assembly of geometric macrocycle isomers. Reproduced with permission.<sup>[54]</sup> Copyright 2016, Wiley-VCH. f) 2D homochirality of porous molecular networks at the liquid–solid interface. Reproduced with permission.<sup>[57]</sup> Copyright 2019, Wiley-VCH.

honeycomb networks as a result of removal of steric hindrance by sequence modification. This approach to construct 2D self-assembly on the flat surfaces provides further insight to construct chiral materials using oligo- and polypeptides as large, multifunctional bio-organic building blocks.

### 3.2. Chiral Induction Synthesis

In addition to the direct synthesis methods, breaking mirror symmetry arranging between achiral building blocks will lead to chirality induction in self-assembly. This idea gives an innovative opportunity to manipulate achiral unit in asymmetric order in the presence of chiral inductors or chiral ligands to construct chiral 2D materials, which called chiral induction synthesis.<sup>[48]</sup>

2D transition metal dichalcogenides (TMDs) materials as the semiconductors have shown a wide applications in spintronics and electronic devices due to the combination of ultrathin thickness, extraordinary nonlinearities, and direct bandgaps.<sup>[49,50]</sup> Among the family of TMDs, MoS<sub>2</sub> particularly gathered attention because of their robustness. Recently, Gun'ko and co-workers used sonication-assisted exfoliation in the presence of chiral ligand (cysteine and penicillamine) in water, enabling to produce chiral MoS<sub>2</sub> nanosheets (Figure 2b). The perfect match between the theoretically calculated results and circular dichroism (CD) spectra indicates that the chirality of nanosheets arises from folding in preferential direction induced by chiral ligands. The result for construction of chiral 2D TMDs offers the opportunities for development of chiroptical sensors and highly efficient selective membrane for enantiomeric separation.<sup>[51]</sup>

Ligand induced strategy is also suitable for construction of 2D hybrid organic–inorganic lead halide perovskites, which are potential applications in circularly polarized light (CPL) and spintronic devices due to the mesmerizing optoelectronic properties.<sup>[52]</sup> Recently, Li and co-workers synthesized chiral 2D perovskites by incorporating the chiral ligand  $\alpha$ -methylbenzylamine (MBA), which shows a high degree of the circularly polarized photoluminescence (PL) and sensitive CPL detection (Figure 2c). The chiral 2D perovskites were synthesized by a solution method in the presence of enantiomerically pure chiral ligand, *S*-MBA or *R*-MBA. The chirality is considered to arise from the lattice distortion and/or temperature dependent spin flipping. In the case of (*S*-MBA)<sub>2</sub>PdI<sub>4</sub>, a maximum degree of the circularly polarized PL of 17.6% was observed.<sup>[53]</sup>

In addition to the static chiral sheet architectures, dynamic sheets such as rolling to form curved structures upon external stimuli with chirality switching have recently been reported. In 2017, Lee and co-workers constructed self-sorted static and dynamic chiral sheets through selective self-assembly of geometric *cis* and *trans* macrocycle isomers based on anthracene units with side chiral oligoether dendrons, in which the *trans* isomer forms dynamic rolling sheets that are reversibly unrolled upon thermal treatment (Figure 2e).<sup>[54]</sup> While the *cis* isomer forms static 2D sheets with a lack of thermal responsibility. Both sheets are formed via lateral association of primary nanofibers, and the chiral nature originates from different

mechanisms. In the case of the *cis*-isomer, the chirality induces by a twist conformation of molecular building block. On the other hand, the *trans*-isomer gives rise to a chiral sheet structures by packing induced chirality between the adjacent anthracene units. Consequently, the twisted packing of the adjacent intermolecular anthracene moieties generates rolled sheets at room temperature. Upon heating, the rolled sheets transform into open sheets with dramatic decreasing in the CD intensities, indicating that the overlapped packings of anthracene moieties drive unfolded state of the sheets to relieve the enthalpic penalty caused by thermal dehydration of oligoether chains. To further understand the direction of rolling-up, Jung and co-workers constructed rollable sheet architectures through self-assembly of achiral glycine-appended bipyridine derivatives, the rolling direction can be tuned via addition chiral calix[4]arene analogs.<sup>[55]</sup>

Self-assembly on the surfaces or interfaces is another topic to construct chiral 2D supramolecular architectures. Tobe and co-workers synthesized a series of alkoxy-substituted dehydrobenzo[12]annulene derivatives to construct the on-substrate 2D-assemblies.<sup>[35,56]</sup> When the building blocks assemble on the surface, the 2D confined space drives different arrangements of the side chains, in which the chirality is generated by asymmetric orientation of intermolecular interdigitation patterns. Homochiral supramolecular chiral pores can be demonstrated either utilizing chiral side chains or induced by chiral guest (Figure 2f).<sup>[57]</sup> Unfortunately, up to now, these monolayered chiral porous assemblies have not shown successful examples for further potential applications, but the strategy for construction of the supramolecular chiral pores will offer grand potentials to show good performance for chiral absorption due to extremely large surface area.<sup>[58]</sup>

### 3.3. Postmodification

As mentioned above, not only semiconductors attracted interests for optoelectronic devices but graphene-based materials showed great attraction for excellent optical and electronic properties. The induction of chirality of graphene materials is expected to enrich fascinating physical and chemical phenomena. Because the robust carbon frameworks linked by covalent bond through sp<sup>2</sup> orbitals with ordered period in large scale, postmodification provides the opportunity by using chemical modifications of the chiral moiety depending on demand into the achiral parent architectures. Kotov's group reported that construction of chiral graphene quantum dots (GQDs) are based on the covalent edge modification with cysteine moieties (Figure 2d). First, asymmetric GQDs were prepared through chemical oxidation and cutting of micrometer-sized pitch-based carbon fibers as the "top-down" strategy, then *L*- or *D*-cysteine moieties were bound to the edges of the sheets through amide bonds. The collective interactions of cysteine with graphene via amide bonds induce the twist conformation of the graphene sheets, which reflects in a new cotton effect at 250–265 nm in CD spectrum. The strong luminescence and surface-enhanced Raman spectroscopy of the GQDs demonstrate the possibility of circular polarization effects in both photoluminescence and Raman scattering. Notably, this chiral GQDs show high biocompatibility with liver

cell and D-GQDs shows the strong binding capability with cellular membrane, indicating the potential applications for drug delivery vehicles.<sup>[59]</sup> In the same year, Martín group reported the chiral oxides GQDs via esterification with enantiomerically pure 2-phenyl-1-propanol, and the chirality of oxides GQDs can be transferred to the supramolecular assembly, which induces chiral stacking of pyrene molecules.<sup>[60]</sup>

#### 4. 2D Chiral Porous Materials with Pore Functions

Owing to the interesting potential applications in guest adsorbents or separators, catalysts, optoelectronics, and chemical sensings, tremendous efforts have been spared to discovery of 2D

porous materials with functionalized interiors. The defined design of the 2D porous materials gives excellent pore performance due to the intrinsic properties like robust skeleton, periodic, and uniform pore size with large surface area. After modifying the chiral property of the pore, 2D chiral porous materials have shown fantastic instances in heterogeneous asymmetric catalysis,<sup>[61]</sup> chiral separations,<sup>[62]</sup> and chiroptical devices.<sup>[50]</sup>

2D MOFs with homochirality as emerging chiral materials have attracted intense interest because the pores are able to be functionalized for asymmetric catalysis and enantioselective separations. In 2014, Cui and co-workers synthesized two isostructural chiral MOFs from enantiopure tetracarboxylate-bridging ligands of 1,10-biphenol, in which the chirality arises from the axis chirality of the biphenols (Figure 3a). The large chiral pore

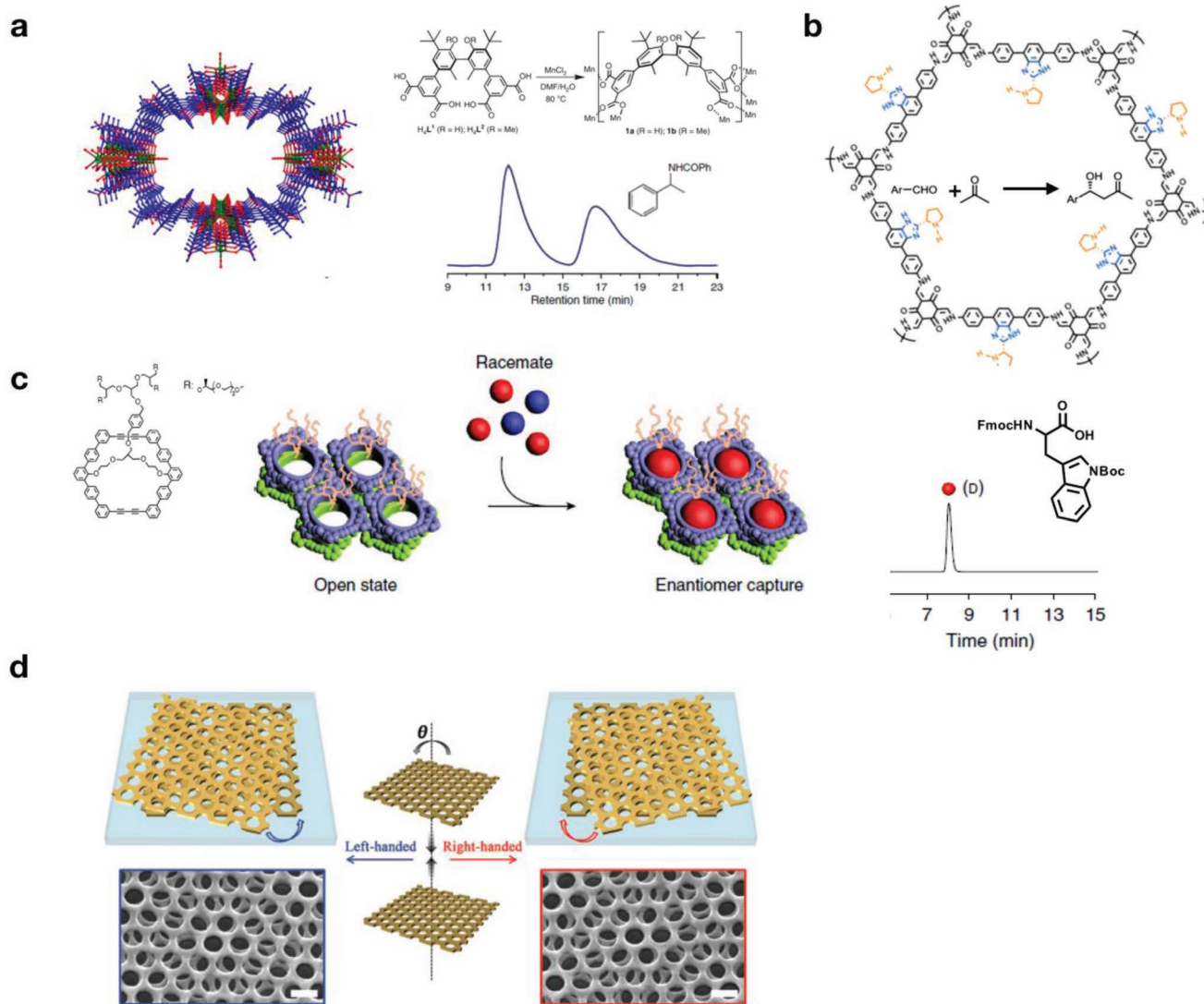


**Figure 3.** Schematic representation of 2D chiral porous materials with pore functions. a) Enantiomeric separation of benzyl amine by Chiral MOF as the stationary phase of chiral HPLC. Reproduced with permission.<sup>[63]</sup> Copyright 2014, Springer Nature. b) Chiral-pyrrolidine-based chiral COF functioned as heterogeneous catalyst for asymmetric aldol reaction. Reproduced with permission.<sup>[64]</sup> Copyright 2016, American Chemical Society. c) Homochiral porous sheets from lateral-associated macrocyclic amphiphile dimers as size-sensitive and enantioselective adsorbents. Reproduced with permission.<sup>[65]</sup> Copyright 2018, Springer Nature. d) Moiré chiral metamaterials with tunable chiroptical responses via chiral stacking of two layers of Au nanoporous. Reproduced with permission.<sup>[69]</sup> Copyright 2017, Wiley-VCH.

size and the chiral dihydroxyl groups from biphenols suggest that this MOF can be a candidate for enantioselective adsorption and separation. 1-Phenylethylamine (1-PEA) was selected as a model compound because the MOF shows excellent absorbent of amines. To evaluate the performance of chiral separation, evacuated *S*-form of MOF crystals were immersed in racemic 1-PEA in different solvents. The optimized condition was found in MeOH at  $-10\text{ }^{\circ}\text{C}$ , allowing 91.0% *ee* with the *R*-enantiomer being in excess. Then the electronic and steric properties of guest were investigated in a series of aromatic amines, the *para* position substituted one with an electron withdrawing group gives rise to the excellent enantioselectivity. The chiral MOF also shows excellent performance of chiral resolution for amines as the stationary phase of chiral column, in which chiral MOF was packed in a column for high-performance liquid chromatography (HPLC) separation. Combined experimental and simulation results, the chiral recognition and separation arise from different orientations and binding energies of two enantiomer within the chiral microenvironment of the MOFs.<sup>[63]</sup>

To be utilized as an asymmetric catalyst, the skeletons and pores should maintain their chiral integrity in a reaction condition. However, MOFs are based on pH-sensitive coordination interactions between ligands and central metals, which limit MOFs to be fulfilled in a wide range of pH conditions. In contrast, COFs show good tolerances even in strong acidic or basic conditions because the building blocks are connected by robust covalent bonds. Wang and co-workers constructed two chiral COFs named as LZU-72 and LZU-76 which were synthesized via imine condensation by chiral-pyrrolidine moiety modified amino linkers.<sup>[64]</sup> After cleavage of the *t*-butyloxy carbonyl protective groups, the chiral reactive moieties stably located on the wall of the pores. In contrast to LZU-72, LZU-76 shows higher stability in acidic conditions due to the  $\beta$ -ketoamine linkages. Accordingly, LZU-76 was selected to characterize the asymmetric aldol reactions with a series of aromatic aldehydes and acetones to form chiral alcohols in the presence of trifluoroacetic acid. Compared with homogeneous catalyst (*S*)-4,7-diphenyl-2-(pyrrolidin-2-yl)-1H-benzo-[d]imidazole, LZU-76 shows a comparable reaction yield and enantioselectivity with much easier recovery method (Figure 3b). Although some successful examples have been reported, the results of chiral COFs in asymmetric catalysis are still rare and expected to further develop. Besides these, chiral pores generated from supramolecular assembly are currently underway, considering great potentials for asymmetric catalyzing chiral reaction.

Despite the chirality inside the pores, the chiral MOFs or COFs are difficult to hinder the stacking between the single framework layers, resulting in pore deformation and low efficiency of the pore performance. In this respect, single-layered porous sheets can be an ideal candidate for allowing the possibility of the perfect pore performance in entrapping substrates because all pores are exposed to the external environments. Inspired by the nanosheets constructed by lateral associated slipped macrocyclic dimer of the amphiphiles,<sup>[38]</sup> Lee group reported the homochiral nanosheets through self-assembly of preferential twist stacking of macrocyclic amphiphiles which shows excellent pore performance in the separation of amino acid guests (Figure 3c).<sup>[65]</sup> The macrocyclic building blocks are stacked to form a twisted dimer due to the nonplanar

conformation of the macrocyclic segments, which generates pore chirality due to symmetry breaking. The resulting dimers laterally associate to form single-layered, homochiral porous sheet structures. The homochirality of the pores can be controlled by chiral transfer from face-on grafted chiral dendritic chains. The chirality and the twist angle were characterized by CD and 2D rotating frame nuclear Overhauser effect spectroscopy experiments. The chirality of the pores is based on the fixed molecular conformation, so that the chiral sheets can be utilized as enantiomer sieving materials for chiral separation of racemic amino acid guests. Hydrophobically protected tryptophan was selected because the hydrophobic aromatic pore were compatible with the guest size. Upon addition the racemic mixture of guests into the methanol solution of chiral sheets, the pores showed greater than 96% uptake capacity. Notably, chiral HPLC was performed consequently, and the encapsulated guest showed to be optically pure without any trace of the other enantiomer, indicating that the chiral sheets exclusively capture one enantiomer from its racemic mixture solution. Upon addition of salts, the hydrated oligoether chains are hydrophobically collapsed to block the pores with simultaneously pumping out the captured guests from the porous sheets. The reformed chiral porous sheet structures perform repeated enantiomer uptake and release cycles. When a series of guests with different molecular sizes were investigated, only the guest molecules with compatible size can be encapsulated, indicative of remarkable size selectivity. Considering the advantages of membrane technology such as easy to scale-up and save energy, the membrane structures can be continuously operated with high efficiency, which fulfil the need for commercial-scale preparation of enantiomerically pure substances.<sup>[66–68]</sup> 2D Porous sheets with homochiral pores as a promising chiral membrane may pave the way to realize continuous separation of enantiomers in a racemic solution.

Although the homochiral porous sheets have shown excellent performance for chiral separation and good stability because the pore is fixed by molecular conformation, there are still obvious limitations for the separation of different sizes of guest molecules due to a fixed, covalent macrocycle pore. A promising solution would be the construction of noncovalent chiral pore with a flexible pore size need to be investigated further.

If we extend the definition of “guest” to light, which changes the optical properties including phase, frequency, and chiral rotation, chiral metamaterials and metasurfaces such as plasmonic chiral metamaterials, moiré chiral metamaterials and transition metal dichalcogenides metasurfaces can be constructed. For example, Wu and Zheng developed a moiré chiral metamaterials constructed by twist stacking of two layers of Au nanoporous sheets (Figure 3d).<sup>[69]</sup> However, the detailed overview of recent advances in chiral plasmonic 2D metamaterials have already been covered in several reviews,<sup>[70,71]</sup> which is beyond the scope here.

## 5. Conclusion and Perspective

We have given an overview of current advances in the development of supramolecular 2D chiral materials and their

applications. There are mainly three ways to introduce the chiral properties into 2D architectures through direct synthesis, chiral induction by self-assembly, and postmodification strategy. The unique structural properties of the 2D chiral materials offer their great promise for using in enantiomeric separation, asymmetric catalysis, and optoelectronic devices. Among these applications, the most prominent is the potential for production of optically active macromolecules with the efficient utilization of the chiral microenvironment. For this purpose, the construction of the robust chiral 2D architectures with uniform supramolecular pores will be the crucial factor.

Furthermore, we expect that the recent advances in the preparation and characterization of 2D chiral materials will provide a platform for macroscopic fabrication of ultrathin chiral materials and pave the way for a breakthrough in chiroptical technology. In addition, the uniform-sized chiral pores in the case of single-layered chiral sheets can be used as chiral nano-reactors based on catch and release protocol.<sup>[72,73]</sup> When achiral substrates are confined in a chiral cavity, the substrate will adopt a fixed chiral conformation, so that chemical transformation will generate chiral product without the use of chiral catalysts. We anticipate that such a purely geometric approach for chiral synthesis will provide a new insight into 2D chiral materials enabling chiral transformation without the help of any chiral moieties, which remains a great challenge.

## Acknowledgements

This work was supported by the National Natural Science Foundation of China (21634005 and 51473062), the National Research Foundation of Korea (NRF-2019R1C1C1008526 and NRF-2019R1A4A1027627), and the KU-KIST Research Fund.

## Conflict of Interest

The authors declare no conflict of interest.

## Keywords

2D chiral materials, 2D porous materials, supramolecular materials

Received: August 31, 2019

Revised: December 16, 2019

Published online:

- [1] K. Maeda, E. Yashima, *Top. Curr. Chem.* **2017**, *375*, 72.
- [2] L. Ma, J. M. Falkowski, C. Abney, W. Lin, *Nat. Chem.* **2010**, *2*, 838.
- [3] H. Kim, S. Lee, T. J. Shin, E. Korblova, D. M. Walba, N. A. Clark, S. B. Lee, D. K. Yoon, *Proc. Natl. Acad. Sci. USA* **2014**, *111*, 14342.
- [4] E. Yashima, N. Ousaka, D. Taura, K. Shimomura, T. Ikai, K. Maeda, *Chem. Rev.* **2016**, *116*, 13752.
- [5] E. Yashima, K. Maeda, H. Lida, Y. Furusho, K. Nagai, *Chem. Rev.* **2009**, *109*, 6102.
- [6] M. Heitbaum, F. Glorius, I. Escher, *Angew. Chem., Int. Ed.* **2006**, *45*, 4732.
- [7] G. Szöllösi, *Catal. Sci. Technol.* **2018**, *8*, 389.
- [8] C. Tan, D. Chu, X. Tang, Y. Liu, W. Xuan, Y. Cui, *Chem. - Eur. J.* **2019**, *25*, 662.
- [9] J. Shen, Y. Okamoto, *Chem. Rev.* **2016**, *116*, 1094.
- [10] J. S. Seo, D. Whang, H. Lee, S. I. Jun, J. Oh, Y. J. Jeon, K. Kim, *Nature* **2000**, *404*, 982.
- [11] X. Han, J. Zhang, J. Huang, X. Wu, D. Yuan, Y. Liu, Y. Cui, *Nat. Commun.* **2018**, *9*, 1294.
- [12] Z. Huang, S.-K. Kang, M. Banno, T. Yamaguchi, D. Lee, C. Seok, E. Yashima, M. Lee, *Science* **2012**, *337*, 1521.
- [13] Y. Kim, J. Kang, B. Shen, Y. Wang, Y. He, M. Lee, *Nat. Commun.* **2015**, *6*, 8650.
- [14] C. S. Cundy, P. A. Cox, *Chem. Rev.* **2003**, *103*, 663.
- [15] K. S. Novoselov, Z. Jiang, Y. Zhang, S. V. Morozov, H. L. Stormer, U. Zeitler, J. C. Maan, G. S. Boebinger, P. Kim, A. K. Geim, *Science* **2007**, *315*, 1379.
- [16] A. K. Geim, *Science* **2009**, *324*, 1530.
- [17] S.-L. Cai, W.-G. Zhang, R. N. Zuckermann, Z.-T. Li, X. Zhao, Y. Liu, *Adv. Mater.* **2015**, *27*, 5762.
- [18] E. Lee, J.-K. Kim, M. Lee, *Angew. Chem., Int. Ed.* **2009**, *48*, 3657.
- [19] S. Shin, S. Lim, Y. Kim, T. Kim, T.-L. Choi, M. Lee, *J. Am. Chem. Soc.* **2013**, *135*, 2156.
- [20] Y.-b. Lim, E. Lee, Y.-R. Yoon, M. S. Lee, M. Lee, *Angew. Chem., Int. Ed.* **2008**, *47*, 4525.
- [21] Y.-b. Lim, O.-j. Kwon, E. Lee, P.-H. Kim, C.-O. Yun, M. Lee, *Org. Biomol. Chem.* **2008**, *6*, 1944.
- [22] S.-Y. Jiang, X. Zhao, *Chin. J. Polym. Sci.* **2019**, *37*, 1.
- [23] R. Sekiya, Y. Uemura, H. Murakami, T. Haino, *Angew. Chem., Int. Ed.* **2014**, *53*, 5619.
- [24] S. Das, P. Heasman, T. Ben, S. Qiu, *Chem. Rev.* **2017**, *117*, 1515.
- [25] Y. Song, Q. Sun, B. Aguila, S. Ma, *Adv. Sci.* **2019**, *6*, 1801410.
- [26] Y. Liu, W. Xuan, Y. Cui, *Adv. Mater.* **2010**, *22*, 4112.
- [27] I. Hisaki, C. Xin, K. Takahashi, T. Nakamura, *Angew. Chem., Int. Ed.* **2019**, *58*, 11160.
- [28] S.-L. Cai, W.-G. Zhang, R. N. Zuckermann, Z.-T. Li, X. Zhao, Y. Liu, *Adv. Mater.* **2015**, *27*, 5726.
- [29] D. J. Ashworth, J. A. Foster, *J. Mater. Chem. A* **2018**, *6*, 16292.
- [30] M. S. A. Bhuyan, M. N. Uddin, M. M. Islam, F. A. Bipasha, S. S. Hossain, *Int. Nano Lett.* **2016**, *6*, 65.
- [31] K. S. Novoselov, A. K. Geim, S. V. Morozov, D. Jiang, Y. Zhang, S. V. Dubonos, I. V. Grigorieva, A. A. Firsov, *Science* **2004**, *306*, 666.
- [32] M. J. Allen, V. C. Tung, R. B. Kaner, *Chem. Rev.* **2010**, *110*, 132.
- [33] D.-W. Lee, T. Kim, M. Lee, *Chem. Commun.* **2011**, *47*, 8259.
- [34] B. Shen, Y. He, Y. Kim, Y. Wang, M. Lee, *Angew. Chem., Int. Ed.* **2016**, *55*, 2382.
- [35] X. Liu, H. Li, Y. Kim, M. Lee, *Chem. Commun.* **2018**, *54*, 3102.
- [36] Y. Kim, X. Liu, H. Li, M. Lee, *Chem. - Asian J.* **2019**, *14*, 952.
- [37] J.-K. Kim, E. Lee, Y.-H. Jeong, J.-K. Lee, W.-C. Zin, M. Lee, *J. Am. Chem. Soc.* **2007**, *129*, 6082.
- [38] Y. Kim, S. Shin, T. Kim, D. Lee, C. Seok, M. Lee, *Angew. Chem., Int. Ed.* **2013**, *52*, 6426.
- [39] S. Fa, T. Kakuta, T.-a. Yamagishi, T. Ogoshi, *CCS Chem.* **2019**, *1*, 50.
- [40] T. Ogoshi, K. Yoshikoshi, R. Sueto, H. Nishihara, T. Yamagishi, *Angew. Chem., Int. Ed.* **2015**, *54*, 6466.
- [41] N. Cheng, Y. Chen, X. Wu, Y. Liu, *Chem. Commun.* **2018**, *54*, 6284.
- [42] F. Zaera, *Chem. Soc. Rev.* **2017**, *46*, 7374.
- [43] K.-D. Zhang, J. Tian, D. Hanifi, Y. Zhang, A. C.-H. Sue, T.-Y. Zhou, L. Zhang, X. Zhao, Y. Liu, Z.-T. Li, *J. Am. Chem. Soc.* **2013**, *135*, 17913.
- [44] M. Pfeiffermann, R. Dong, R. Graf, W. Zajaczkowski, T. Gorelik, W. Pisula, A. Narita, K. Müllen, X. Feng, *J. Am. Chem. Soc.* **2015**, *137*, 14525.
- [45] S.-Q. Xu, X. Zhang, C.-B. Nie, Z.-F. Pang, X.-N. Xu, X. Zhao, *Chem. Commun.* **2015**, *51*, 16417.
- [46] X. Chen, Y. He, Y. Kim, M. Lee, *J. Am. Chem. Soc.* **2016**, *138*, 5773.
- [47] S. Abb, L. Harnau, R. Gutzler, S. Rauschenbach, K. Kern, *Nat. Commun.* **2016**, *7*, 10335.
- [48] M. Liu, L. Zhang, T. Wang, *Chem. Rev.* **2015**, *115*, 7304.

- [49] S. Manzeli, D. Ovchinnikov, D. Pasquier, O. V. Yazyev, A. Kis, *Nat. Rev. Mater.* **2017**, 2, 17033.
- [50] G. Hu, X. Hong, K. Wang, J. Wu, H.-X. Xu, W. Zhao, W. Liu, S. Zhang, F. Garcia-Vidal, B. Wang, P. Lu, C.-W. Qiu, *Nat. Photonics* **2019**, 13, 467.
- [51] F. Purcell-Milton, R. McKenna, L. J. Brennan, C. P. Cullen, L. Guillemeney, N. V. Tepliakov, A. S. Baimuratov, I. D. Rukhlenko, T. S. Perova, G. S. Duesberg, A. V. Baranov, A. V. Fedorov, Y. K. Gun'ko, *ACS Nano* **2018**, 12, 954.
- [52] G. Long, C. Jiang, R. Sabatini, Z. Yang, M. Wei, L. N. Quan, Q. Liang, A. Rasmita, M. Askerka, G. Walters, X. Gong, J. Xing, X. Wen, R. Quintero-Bermudez, H. Yuan, G. Xing, X. R. Wang, D. Song, O. Voznyy, M. Zhang, S. Hoogland, W. Gao, Q. Xiong, E. H. Sargent, *Nat. Photonics* **2018**, 12, 528.
- [53] J. Ma, C. Fang, C. Chen, L. Jin, J. Wang, S. Wang, J. Tang, D. Li, *ACS Nano* **2019**, 13, 3659.
- [54] Y. Wang, Y. Kim, M. Lee, *Angew. Chem., Int. Ed.* **2016**, 55, 13122.
- [55] H. Choi, K. J. Cho, H. Seo, J. Ahn, J. Liu, S. S. Lee, H. Kim, C. Feng, J. H. Jung, *J. Am. Chem. Soc.* **2017**, 139, 17711.
- [56] K. Tahara, H. Yamaga, E. Ghijsens, K. Inukai, J. Adisojojoso, M. O. Blunt, S. De Feyter, Y. Tobe, *Nat. Chem.* **2011**, 3, 714.
- [57] K. Tahara, A. Noguchi, R. Nakayama, E. Ghijsens, S. De Feyter, Y. Tobe, *Angew. Chem., Int. Ed.* **2019**, 58, 7733.
- [58] Y. Fang, K. Tahara, O. Ivasenko, Y. Tobe, S. De Feyter, *J. Phys. Chem. C* **2018**, 122, 8228.
- [59] N. Suzuki, Y. Wang, P. Elvati, Z.-B. Qu, K. Kim, S. Jiang, E. Baumeister, J. Lee, B. Yeom, J. H. Bahng, J. Lee, A. Violi, N. A. Kotov, *ACS Nano* **2016**, 10, 1744.
- [60] M. Vázquez-Nakagawa, L. Rodríguez-Pérez, M. A. Herranz, N. Martín, *Chem. Commun.* **2016**, 52, 665.
- [61] X. Chen, Y. Peng, X. Han, Y. Liu, X. Lin, Y. Cui, *Nat. Commun.* **2017**, 8, 2171.
- [62] H.-L. Qian, C.-X. Yang, X.-P. Yan, *Nat. Commun.* **2016**, 7, 12104.
- [63] Y. Peng, T. Gong, K. Zhang, X. Lin, Y. Liu, J. Jiang, Y. Cui, *Nat. Commun.* **2014**, 5, 4406.
- [64] H.-S. Xu, S.-Y. Ding, W.-K. An, H. Wu, W. Wang, *J. Am. Chem. Soc.* **2016**, 138, 11489.
- [65] B. Sun, Y. Kim, Y. Wang, H. Wang, J. Kim, X. Liu, M. Lee, *Nat. Mater.* **2018**, 17, 599.
- [66] R. Xie, L.-Y. Chu, J.-G. Deng, *Chem. Soc. Rev.* **2008**, 37, 1243.
- [67] C. Fernandes, M. E. Tiritan, M. M. M. Pinto, *Symmetry* **2017**, 9, 206.
- [68] X. Weng, J. E. Baez, M. Khiterer, M. Y. Hoe, Z. Bao, K. J. Shea, *Angew. Chem., Int. Ed.* **2015**, 54, 1121.
- [69] Z. Wu, Y. Zheng, *Adv. Opt. Mater.* **2017**, 5, 1700034.
- [70] V. K. Valev, J. J. Baumberg, C. Sibilica, T. Verbiest, *Adv. Mater.* **2013**, 25, 2517.
- [71] M. Pu, X. Ma, X. Li, Y. Guo, X. Luo, *J. Mater. Chem. C* **2017**, 5, 4361.
- [72] M. Yoshizawa, M. Tamura, M. Fujita, *Science* **2006**, 312, 251.
- [73] J. Li, S. G. Ballmer, E. P. Gillis, S. Fujii, M. J. Schmidt, A. M. E. Palazzolo, J. W. Lehmann, G. F. Morehouse, M. D. Burke, *Science* **2015**, 347, 1221.